IBRO Neuroscience Reports 18 (2025) 830–843

Contents lists available at ScienceDirect

IBRO Neuroscience Reports

journal homepage: www.sciencedirect.com/journal/IBRO-Neuroscience-Reports

Toxoplasma TgCtwh3 Δ*rop16*$_{I/III}$ accelerates neuronal apoptosis and APP production in mouse with acute infection

Di Yang [a,b], Cong Wang [a], Qing Tao [c], Lei Liu [d], Mengmeng Jin [e], Haiping Cai [f], Meijuan Zheng [g], Mengtao Gong [g], Li Yu [h], Jian Du [i], Qingli Luo [a], Jilong Shen [a], Kunpeng Qin [b,*], Deyong Chu [a,*]

[a] *Department of Pathogen Biology, Anhui Province Key Laboratory of Microbiology & Parasitology, Anhui Provincial Laboratory of Zoonoses of High Institutions, School of Basic Medicine, Anhui Medical University, Hefei, China*
[b] *Department of Orthopaedics, The First Affiliated Hospital of Anhui Medical University. Anhui Public Health Clinical Center, Hefei, China*
[c] *Department of Laboratory Medicine, Affiliated Drum Tower Hospital, Nanjing University School of Medicine, Nanjing, China*
[d] *Department of Blood Transfusion, the First Affiliated Hospital of USTC, Division of Life Sciences and Medicine, University of Science and Technology of China, Hefei, China*
[e] *Maternity and Child Health Hospital of Anhui Province, the Affiliated Maternity and Child Health Hospital of Anhui Medical University, Hefei, China*
[f] *Spine center, Department of Orthopaedics, The First Affiliated Hospital of USTC, Division of Life Sciences and Medicine, University of Science and Technology of China, Hefei, China*
[g] *Department of Laboratory Medicine, the First Affiliated Hospital of Anhui Medical University, Hefei, China*
[h] *Department of Microbiology and Parasitology, Anhui Provincial Laboratory of Microbiology and Parasitology, Anhui Provincial Laboratory of Zoonoses of High Institutions, School of Basic Medical Sciences, Anhui Medical University, Hefei, China*
[i] *Department of Biochemistry and Molecular Biology, School of Basic Medical Sciences, Anhui Medical University, Hefei, China*

ARTICLE INFO

Keywords:
T.gondii Chinese 1 genotype Wh3 strain
ROP16$_{I/III}$
Hippocampal neuron
Apoptosis
APP

ABSTRACT

Objective: To explore the mechanism by which *rop16*$_{I/III}$-deficient/*gra15*$_{II}$-dominant *toxoplasma gondii* Chinese 1 genotype Wh3 (TgCtwh3 Δ*rop16*$_{I/III}$) strain induced neuron apoptosis, APP and BACE1 production *in vivo* and *vitro*.

Method: BALB/c mice were infected by intraperitoneal injection with TgCtwh3 wild type (TgCtwh3 WT) and TgCtwh3 Δ*rop16*$_{I/III}$ tachyzoites, respectively. One week after infection, the morphology and number of hippocampal neurons were examined by hematoxylin-eosin (H&E) and Nissl staining. Expression levels of apoptosis-related proteins, APP, BACE1 as well as inflammatory factors proteins and genes in the hippocampus were evaluated using western blotting and qRT-PCR. The hippocampal neuron cell line HT22 was infected with TgCtwh3 WT and TgCtwh3 Δ*rop16*$_{I/III}$ tachyzoite, respectively, and the expression of target proteins was analyzed through immunofluorescence staining and western blotting. Furthermore, HT22 apoptosis was assessed using flow cytometry.

Result: BALB/c mice injected with TgCtwh3 Δ*rop16*$_{I/III}$ tachyzoites presented abnormal appearance and posture changes as well as declined vitality. The hippocampus assay demonstrated that TgCtwh3 Δ*rop16*$_{I/III}$ *toxoplasma* caused neuron loss, neuron alignment disorder, neuronal nucleus abnormal deep-stained and neuron apoptosis. Furthermore, TgCtwh3 Δ*rop16*$_{I/III}$ tachyzoites caused obvious production of APP, BACE1and expression increase of pro-inflammatory factors in hippocampal tissue compared to these in mice infected with TgCtwh3 WT tachyzoites. Contrarily, the expression of transforming growth factor beta 1 (TGF-β1), a pivotal anti-inflammatory cytokine was significantly decreased in TgCtwh3 Δ*rop16*$_{I/III}$ infected mice. Further study showed that TgCtwh3 Δ*rop16*$_{I/III}$ tachyzoites induced HT22 apoptosis through triggering ERS, meanwhile promoted HT22 to produce APP, BACE1 by activating NF-κB signaling pathway.

Conclusion: Our results indicated that the GRA15$_{II}$ effector may play a crucial part in neuron apoptosis, pro-inflammatory factors secretion, and APP, BACE1 production. Inversely, ROP16$_{I/III}$ effector may play a potentially protective role in this process.

* Corresponding authors.
E-mail addresses: yag0505@163.com (Di Yang), 1334817011@qq.com (C. Wang), 2860432696@qq.com (Q. Tao), liulei7978@126.com (L. Liu), 20881575@qq.com (M. Jin), chpdmy@163.com (H. Cai), zhengmjzh@163.com (M. Zheng), 2792263692@qq.com (M. Gong), lilyyu33@126.com (L. Yu), dujian@ahmu.edu.cn (J. Du), luoqingli98@vip.163.com (Q. Luo), shenjilong53@126.com (J. Shen), qkp200008@126.com (K. Qin), chudeyong@126.com (D. Chu).

https://doi.org/10.1016/j.ibneur.2025.05.009
Received 5 March 2025; Received in revised form 21 May 2025; Accepted 21 May 2025
Available online 24 May 2025

1. Introduction

Neurodegenerative disease is characterized by the loss of neuronal populations and pathological protein aggregation (Dugger and Dickson, 2017). As a multifactorial neurodegenerative condition, pathogenic infections caused by bacteria, viruses, fungi, and parasites may increase the risk of developing Alzheimer's disease (AD) (Piekut et al., 2022). These infections may result in neuroinflammation, the development of β-amyloid (Aβ), and neuronal apoptosis (Zhou et al., 2022). Aβ is the aggregation of misfolded amyloid-β protein that produces Aβ peptides with varying lengths by cleaving the amyloid precursor protein (APP) primarily by two proteases, β-secretase (BACE1) and γ-secretase (Oakley et al., 2006). According to the study, activation of NF-κB signaling can promote pro-inflammatory cytokines, APP and BACE1 up-regulated (Calsolaro and Edison, 2016; Graham and Pragnell, 1990; Kim et al., 2021;Shi et al., 2017), meanwhile, upregulation of BACE1 can activate NF-κB pathway to increase Aβ expression (Guglielmotto et al., 2012).

Toxoplasma gondii (*T gondii*) is an exclusive intracellular parasitic that is capable of affecting almost all vertebrate animals including humans (Dubey et al., 1998; El Saftawy et al., 2020). *T.gondii* can invade brain parenchyma neurons as early as 24 h after it infects mouse (Olivera et al., 2021) and secrete various virulent effectors, including rhoptry protein (ROP), dense granules protein (GRA), and so on (Saeij et al., 2006; Taylor et al., 2006). Type I or III *T.gondii* ROP16 protein (ROP16 $_{I/III}$) could promote the polarization of M2 macrophages through the STAT3/STAT6 pathway and enhance the synthesis of transforming growth factor beta 1 (TGF-β1), and other anti-inflammatory cytokines (Xu et al., 2019). Neuroinflammation has been suggested as a possible mechanism for cognitive impairment (Kinney et al., 2018). Our previous study found that *T.gondii* Chinese 1 genotype Wh6 strain (TgCtwh6) may cause mice abnormal cognitive behavior with the production of pro-inflammatory factors, the increase of APP, BACE1, Aβ and the apoptosis of neurons in hippocampus (Tao et al., 2023). Some studies have reported that astrocytes and microglia, activated through *T.gondii* infections produce a variety of immune effector molecules that can mediate inflammation and neuronal apoptosis, which can lead to neurodegenerative diseases (Caballero et al., 2022). Moreover, these pro-inflammatory cytokines can induce iNOS, NO, BACE1 increase and synapse loss (Calsolaro and Edison, 2016; Catumbela et al., 2023). Type II *T.gondii* GRA15 protein (GRA15$_{II}$) could activate the NF-κB signaling pathway to induce not only macrophage polarization towards the M1 cell phenotype (Jensen et al., 2011), but also cell apoptosis through endoplasmic reticulum stress (ERS) (Wei et al., 2018). The main mechanism of this apoptosis pathway is the unfolded protein response (UPR) (Huang et al., 2022). The immunoglobulin heavy chain-binding protein (BIP), is considered to be the primary chaperone protein in the endoplasmic reticulum (ER) that binds to unfolded proteins and dissociates from membrane-bound ER stress sensors, thereby inhibiting mRNA translation to protect the cell from an excess of unfolded proteins (Liu et al., 2023; Tseng et al., 2019; Vidal et al., 2023). Therefore, elevated BIP expression can serve as an important marker of ERS activation (Pfaffenbach and Lee, 2011). Caspase12 is identified as the first ER-associated member of the cysteinyl aspartate specific proteinase and is activated by ER stress (Nakagawa et al., 2000), then Caspase 12 translocate from the ER membrane to the cytoplasm (Rao et al., 2001), activates downstream apoptotic signals, such as Caspase3 (Nakagawa et al., 2000).

Type Chinese1(ToxoDB #9) stains, TgCtwh3 and TgCtwh6, dominantly prevalent in China carry both GRA15$_{II}$ and ROP16$_{I/III}$ effectors that are different from the stains of archetypical type I, II, III of *T.gondii* prevalent in Europe and America (Cheng et al., 2015; Howe and Sibley, 1995). Chinese 1 strains suggest the distinct neurological pathogenesis that is different from the other strains. Our previous research showed that TgCtwh6, a hypo virulent strain, caused mice chronic infection and cognitive behavior damage with APP, BACE1 production and Aβ aggregation in hippocampal tissue (Tao et al., 2023). But the effect of the virulent strain, TgCtwh3 Δ*rop16*$_{I/III}$ on neuron apoptosis, APP production remains unclear.

We hypothesize that the TgCtwh3 Δ*rop16*$_{I/III}$ strain with *gra15*$_{II}$ background, like type II strains of *toxoplasma*, might induce neuron apoptosis and APP production through activating ERS and NF-κB signaling pathway in acute infection. This study would be helpful for us to better understand of the genotype-associated mechanism of neurodegenerative disease caused by *toxoplasma* predominantly circulates in China.

2. Materials and methods

2.1. Antibodies and materials

Anti-APP, BIP antibodies were purchased from Immunoway (Plano, TX, USA). Anti-BACE1, Bax, Bcl2, Cleaved-caspase3, Cleaved-caspase12, NF-κBp65, *p*-NF-κBp65 antibodies were purchased from Wanleibio (Shenyang, China). FITC-labeled goat anti-rabbit IgG, phenylmethanesulfonyl fluoride (PMSF) and phosphorylated protease inhibitors were purchased from Servicebio (Wuhan, China). Anti-β-actin and goat anti-rabbit antibodies were purchased from Proteintech (Chicago, IL, USA). Tauroursodeoxycholate sodium (Tauroursodeoxycholic acid, TUDCA, an endoplasmic reticulum stress inhibitor, Cat# HY-19696), 4-Methyl-N1-(3-phenylpropyl)-1,2-phenylenediamine (JSH-23, NF-κB activation inhibitor, Cat# HY-13982) were obtained from MedChemExpress (New Jersey, USA).

Dulbecco's modified Eagle's medium (DMEM) and fetal bovine serum (FBS) were obtained from Biological Industries (Palestine). 2-(4-Amidinophenyl)-6-indolecarbamidine dihydrochloride (DAPI) , Penicillin-streptomycin, Annexin V-FITC Apoptosis Detection kit and SDS polyacrylamide gel electrophoresis were purchased from Beyotime (Shanghai, China). Hematoxylin and eosin (H&E), Nissl staining kit were purchased from Sigma (St. Louis, MO, USA). BCA protein assay kit was obtained from Biosharp (Hefei, China). Trizol reagent was purchased from Thermo (MIT, USA). RIPA lysis buffer and nitrocellulose membrane were provided by Millipore (Billerica, MA, USA). Primer Script First Strand cDNA Synthesis Kit and SYBR Premix Ex Taq kit were purchased from Sparkjade (Shandong, China). Hippocampal neuron cell line (HT22) and Vero cell line (Vero) were purchased from Procell Life Science (Wuhan, China). TgCtwh3 Δ*rop16*$_{I/III}$ tachyzoites were gifted by Dr. Cong Wang. TgCtwh3 WT and TgCtwh3 Δ*rop16*$_{I/III}$ tachyzoites were kept in Vero cells, respectively, which were stored at −80℃ in our laboratory (Anhui Province Key Laboratory of Microbiology and Parasitology).

2.2. Animals

Female BABL/c mice, aged 8–10 weeks, were obtained from Hangzhou Ziyuan Experimental Animal Technology Company in Zhejiang, China. These mice were specific pathogen-free (SPF) and had an average weight of 18–20 g. The production permit number for these mice was Scxk 2019–0004. The Chinese National Institute of Health Guide for the Care and Use of Laboratory Animals was strictly followed during the treatment of the mice. The Institutional Review Board of the Institute of Biomedicine at Anhui Medical University approved this animal experiment (permit number: AMU26093628). The mice were housed in a colony room at the Anhui Province Key Laboratory of Microbiology and Parasitology, under controlled conditions of a 12/12-hour circadian rhythm, a temperature of 20 ± 2°C, and a humidity of 45 ± 5 %. The mice were provided with standard chow and pure water ad libitum.

After a one-week settling period, firstly one part of the mice were randomly divided into three groups: control group, TgCtwh3 WT group, and TgCtwh3 Δ*rop16*$_{I/III}$ group, to determine the amount of tachyzoites used in the establishment of mouse acute infection model. The control group was just injected intraperitoneally with 200 μl of normal saline, the TgCtwh3 WT group was injected intraperitoneally with 25, 50, 100,

250, 500, 1000 TgCtwh3 WT tachyzoites in 200 μl of normal saline, respectively, and the TgCtwh3 Δ*rop16*$_{I/III}$ group was injected intraperitoneally with 25, 50, 100, 250, 500, 1000 TgCtwh3 Δ*rop16*$_{I/III}$ tachyzoites in 200 μl of normal saline, respectively. After evaluating the optimal relationship between the number of *toxoplasma* tachyzoites injected into mouse and the production of brain APP, 1000 *toxoplasma* tachyzoites were chosen as the optimal amount to infect mouse in the following experiment.

Then, the other part of the mice was randomly divided into three groups, each containing ten mice: control group, TgCtwh3 WT group, and TgCtwh3 Δ*rop16*$_{I/III}$ group. The control group received an intraperitoneal injection of 200 μl of normal saline, meanwhile, the TgCtwh3 WT group and a TgCtwh3 Δ*rop16*$_{I/III}$ group received an intraperitoneal injection of 1000 TgCtwh3 WT tachyzoites in 200 μl of normal saline and 1000 TgCtwh3 Δ*rop16*$_{I/III}$ tachyzoites in 200 μl of normal saline, respectively. On the 7th day post-infection, all mice were euthanized using an anesthetic (2 % pentobarbital sodium, 0.20 ml/100 g), and their hippocampal tissues were collected for histopathological analysis or protein and gene expression detection.

2.3. T.gondii and cell culture

Tachyzoites of TgCtwh3 WT and TgCtwh3 Δ*rop16*$_{I/III}$ were cultured separately in Vero cells in DMEM medium supplemented with 10 % fetal bovine serum, 1 % penicillin-streptomycin at 37°C and 5 % CO_2.

HT22 were cultured in DMEM medium containing 10 % FBS, 1 % penicillin-streptomycin at 37°C, and 5 % CO_2. The HT22 (1×10^6) were seeded in a 6-well plate and incubated for 12 hours. Subsequently, TgCtwh3 WT tachyzoites (3×10^6) or TgCtwh3 Δ*rop16*$_{I/III}$ tachyzoites (3×10^6) were added to the plate to infect the HT22 for an additional 24 hours. Protein expression of Cleaved-caspase3, Bax, Bcl2, APP, BACE1, and cell apoptosis were analyzed using western blotting, immunofluorescence staining, and flow cytometry assay.

In the experiment aimed at inhibiting ERS by TUDCA, HT22 were inoculated in 12-well plates at a density of 5×10^5 and divided into 6 groups: control group, TUDCA group, TgCtwh3 WT group, TgCtwh3 WT+ TUDCA group, TgCtwh3 Δ*rop16*$_{I/III}$ group, and TgCtwh3 Δ*rop16* $_{I/III}$+ TUDCA group. After 12 hours of culture, HT22 in the TUDCA, TgCtwh3 WT + TUDCA and TgCtwh3 Δ*rop16*$_{I/III}$ + TUDCA group were pretreated with TUDCA (200 μM) (Liu et al., 2020) for 12 hours. Then, the corresponding group was infected with TgCtwh3 WT (1.5×10^6) or TgCtwh3 Δ*rop16*$_{I/III}$ (1.5×10^6) tachyzoites at an MOI (Multiplicity of Infection) of 3. After another 24 hours of culture, HT22 were subjected to western blotting or flow cytometry assay.

In the experiment on inhibition of the NF-κB signaling pathway by JSH-23, HT22 (5×10^5) were inoculated in 12-well plates and divided into six groups: control group, JSH-23 group, TgCtwh3 WT group, TgCtwh3 WT + JSH-23 group, TgCtwh3 Δ*rop16*$_{I/III}$ group, and TgCtwh3 Δ*rop16* $_{I/III}$+ JSH-23 group. After culturing for 12 hours, HT22 in the JSH-23, TgCtwh3 WT + JSH-23, and TgCtwh3 Δ*rop16*$_{I/III}$ + JSH-23 group were pretreated with JSH-23 (10 μM) (Peng et al., 2020) for 12 h. Then, the corresponding group was infected with TgCtwh3 WT (1.5×10^6) or TgCtwh3 Δ*rop16*$_{I/III}$ (1.5×10^6) tachyzoites with MOI= 3. After incubation for another 24 hours, HT22 were subjected to western blotting or immunofluorescence staining.

2.4. Hematoxylin and eosin (HE) staining

Three mice were selected randomly from each group for histopathologic examination of hippocampal tissue. The paraffin sections of hippocampal tissue (4μm) were dewaxed thrice in xylene and then hydrated in different gradient concentrations of ethanol. The dewaxed paraffin sections were treated with hematoxylin for 5 min, rinsed slowly with running water for several seconds, and differentiated with 1 % hydrochloric acid alcohol for 30 s. Subsequently, the sections were rinsed slowly with running water for several seconds and immersed in eosin for 25 s to 1 min. Finally, the sections were dehydrated routinely in anhydrous ethanol, permeabilized in xylene, sealed with neutral resin, and left to dry naturally. All HE-stained tissue sections were examined under a light microscope (LEICA, Wetzlar, Germany) with magnifications of 20 × 10 and 40 × 10. The images in five randomly different fields of view of the hippocampal zone for each section were captured by an observer in a blinded manner.

2.5. Nissl staining

Changes in the number of Nissl bodies within neurons of the hippocampal region of mice infected with TgCtwh3 WT or TgCtwh3 Δ*rop16*$_{I/III}$ tachyzoite were observed through nissl staining. Following dewaxed and hydrated, the paraffin sections were immersed in a tarry violet staining solution at 56°C for 1 h. The dye was slowly rinsed off with deionized water. The sections were then placed in Nissl differentiation solution for 2 min. The degree of differentiation was observed under a microscope. The sections were dehydrated routinely in anhydrous ethanol, permeabilized in xylene, sealed with neutral resin, and left to dry naturally. All sections were observed under an optical microscope (40 ×10) (LEICA, Wetzlar, Germany). The images in five randomly different fields of view of the hippocampal zone for each section were captured by an observer in a blinded manner, and the total number of positive cells was recorded for the final Image J (USA) analysis.

2.6. Immunofluorescence staining

HT22 pretreated or untreated with JSH-23 was infected by TgCtwh3 WT or TgCtwh3 Δ*rop16*$_{I/III}$ tachyzoites in 12-well plates for 24 h then fixed with 4 % paraformaldehyde for 15 min. The cell slides were sealed with immunofluorescent blocking solution for 1 h, then incubated with primary antibody APP (1:200), BACE1 (1:200), NF-κBp65 (1:200), *p*-NF-κBp65 (1:200) at 4°C overnight, and finally incubated with goat anti-rabbit IgG coupled with FITC (1:200) for 1 h at 37°C, followed by counterstaining nuclei with DAPI. The images in five randomly different fields of view for each cell slide were captured by an observer in a blinded manner under a fluorescence microscope (20 ×10 and 40 ×10) (LEICA, Wetzlar, Germany). Finally, they were analyzed with Image J (MD, USA).

2.7. Western blotting

Lysis of approximately 80 mg of hippocampal tissue or cultured HT22 with RIPA lysis buffer supplemented with protease inhibitor. The extracted total protein concentration was then determined using a BCA protein concentration assay kit. Each protein sample (10 μg) was added to a 12.5 % polyacrylamide gel for electrophoresis and separation, and then transferred to a polyvinylidene difluoride membrane (PVDF). Membranes were incubated with APP (1:2000), BACE1 (1:500), Bax (1:1000), Bcl2 (1:500), Cleaved-capsase3 (1:500), Cleaved-caspase12 (1:1500), BIP (1:2000), NF-κBp65 (1:1000), *p*-NF-κBp65 (1:1000) and β-actin (1:5000) primary antibodies overnight at 4°C and then incubated with enzyme-labeled secondary antibodies (1:10,000) at room temperature for 1 h. Specific protein signals were detected with the ECL chemiluminescence kit. The Chemo Dox XRS system (Bio-Rad Laboratories, Hercules, CA, USA) was used to view the images from the blots. The optical density of each band was calculated using the Image J program (MD, USA).

2.8. Quantitative real-time PCR (RT-qPCR)

RNA was extracted from hippocampal tissues with TRIzol reagent, and RNA concentration and purity were determined by NanoDrop2000 (Thermo Scientific, Shanghai, China) software. The RNA was reverse transcribed to cDNA using the primer Script first Strand cDNA Synthesis

Table 1
The primers used for qRT-PCR.

Primers	Forward primer(5'-3')	Reverse primer(5'-3')
IL−6	CCGGAGAGGAGACTTCACAG	CATTTCCACGATTTCCCAGA
TNF-α	ACGGCATGGATCTCAAAGAC	GTGGGTGAGGAGCACGTAGT
iNOS	CACCTTGGAGTTCACCCAGT	ACCACTCGTACTTGGGATGC
TGF-β1	CTGGATACCAACTACTGCTTCAG	TTGGTTGTAGAGGGCAAGGACCT
APP	TGAATGTGCAGAATGGAAAGTG	AACTAGGCAACGGTAAGGAATC
BACE1	GCAGACATGGAAGACTGTGGCTAC	GGCAGAGTGGCAACATGAAGAGG
GAPDH	CAACTTTGGCATTGTGGAAGG	ACACATTGGGGGTAGGAACAC

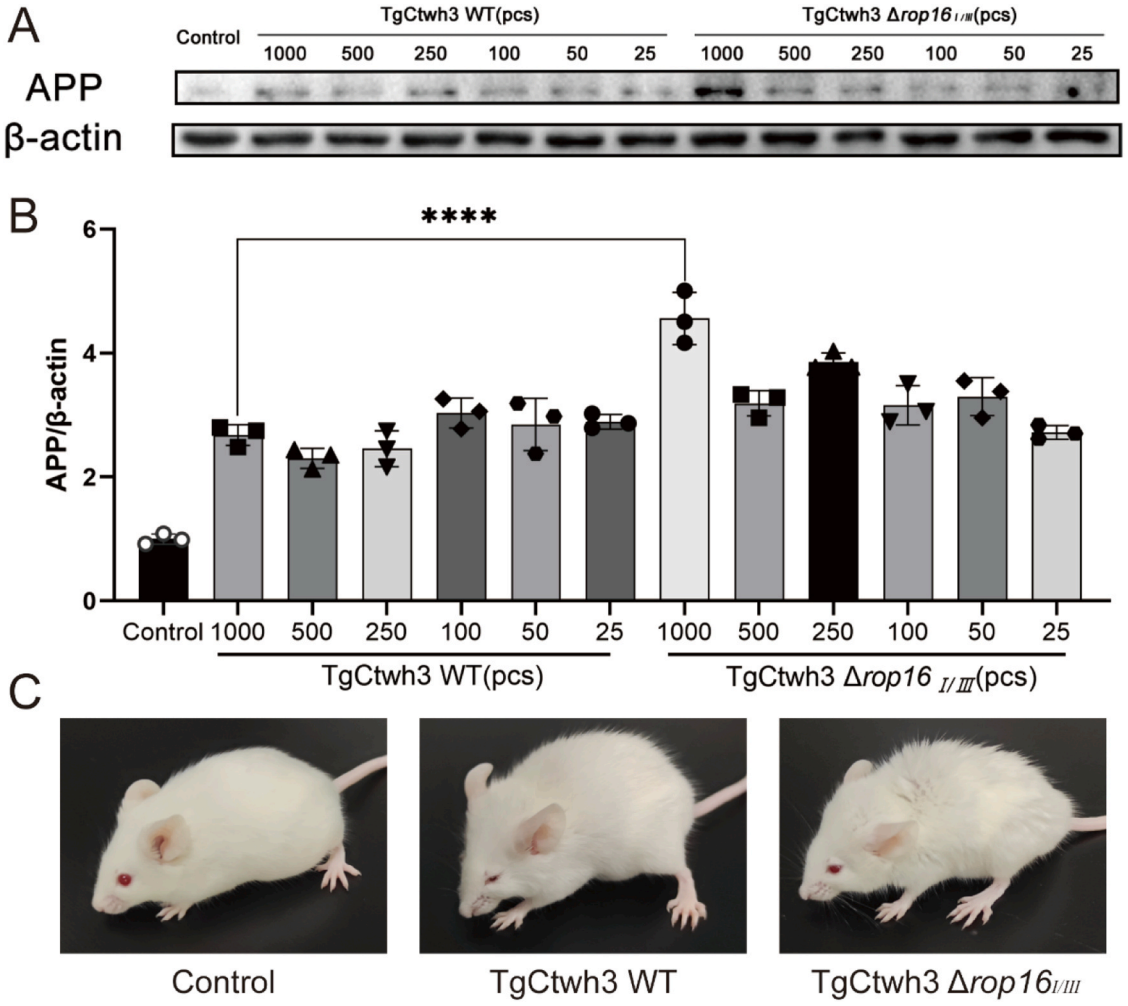

Fig. 1. TgCtwh3 acute infection mice model was established.

Kit. The qRT-PCR was performed using SYBR Premix Ex Taq kit and Light Cycler 96 (Roche, Switzerland) to detect the expression of IL-6, TNF-α, iNOS, TGF-β1, APP and BACE1, and the thermal cycling conditions were programmed following the manufacturer's protocol. The expression of the relevant genes was analyzed by the 2-ΔΔCT method with statistical cycle thresholds. The abundance of target RNA transcripts was evaluated relative quantitatively using the housekeeping gene GAPDH as a control. The gene-specific primer sequences are listed in Table 1.

2.9. Flow cytometry

HT22 pre-treated or non-treated with TUDCA were infected with TgCtwh3 WT or TgCtwh3 Δ*rop16*$_{I/III}$ tachyzoites in 12-well plates for 24 h. Then the HT22 were collected, and HT22 apoptosis was detected by FITC Annexin V Apoptosis Detection Kit and CytoFLEX flow cytometry. Finally, the results were analyzed by FlowJo_V10.

3. Statistical Analysis

All data were obtained from triplicate values representing three independent experiments with identical conditions. One-way ANOVA followed by the Bonferroni post hoc test was used for data analysis using GraphPad Prism 8.2.1 (GraphPad Software, San Diego, CA, USA). All results were assessed as mean ± SD (n = 5 replicates for each group), two-tailed $P < 0.05$ or $P < 0.01$ or $P < 0.001$ or $P < 0.0001$ was regarded as statistically significant.

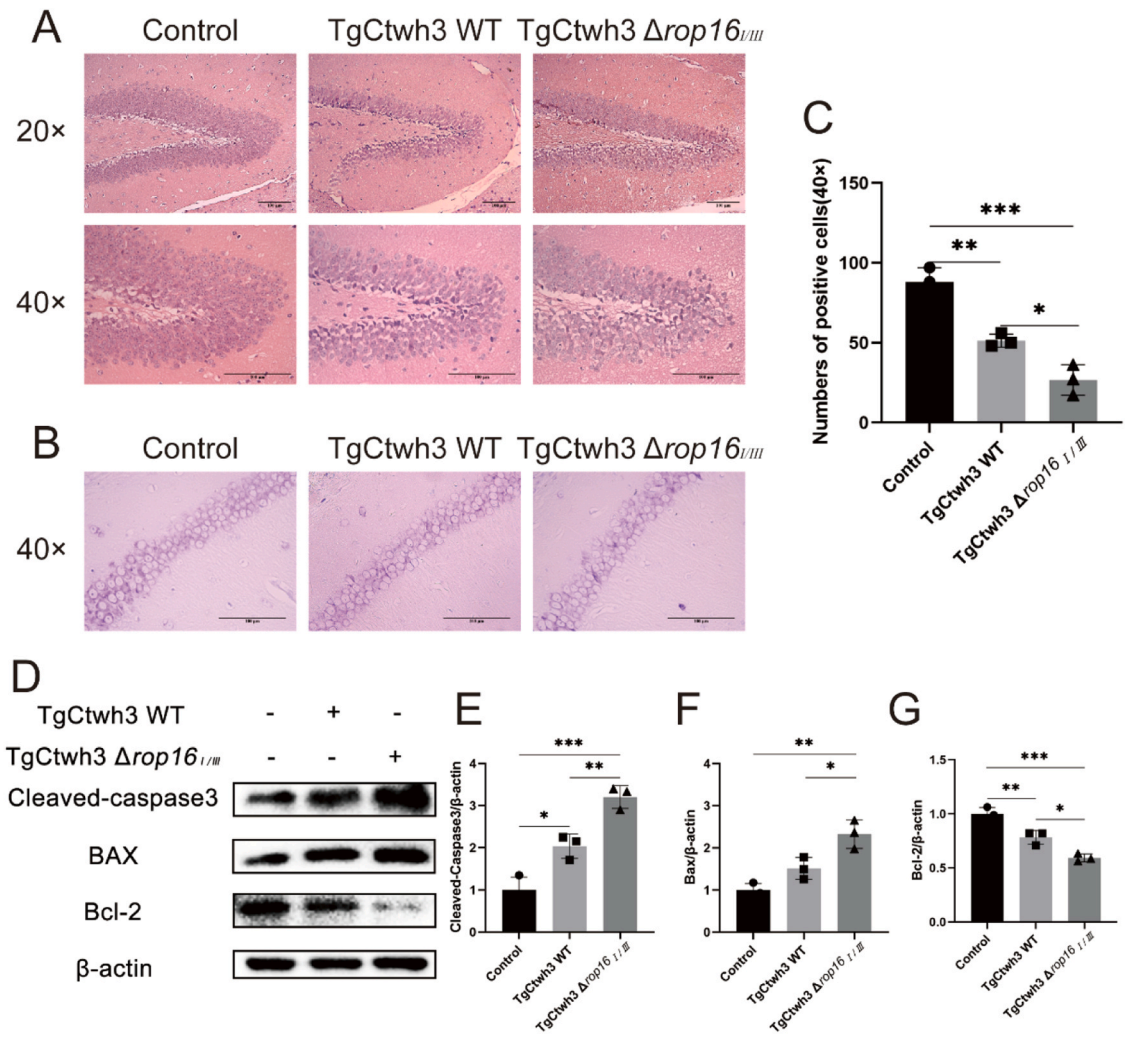

Fig. 2. Hippocampal neuron apoptosis was caused by TgCtwh3 Δ*rop16*$_{I/III}$ infection.

4. Results

4.1. Establishment of the mouse acute infection model

To choose the optimal *toxoplasma* tachyzoites to challenge mouse and establish mouse acute infection model, we first evaluated the optimal relationship between the number of *toxoplasma* tachyzoites injected intraperitoneally into mice and the production of brain APP. One week after injection, western blotting was performed on the hippocampus of mice, and the results showed that the injection of 1000 *toxoplasma* tachyzoites caused an increase at most in APP (Fig. 1A, B). Therefore, mice were infected with 1000 *toxoplasma* tachyzoites to establish mouse acute infection model. The mice infected with TgCtwh3 WT or TgCtwh3 Δ*rop16*$_{I/III}$ showed a typical hunchback posture, uneven fur, stiff limbs, and dull eyes compared to uninfected mice (Fig. 1C).

The mice were randomly divided into three groups. The control group was injected 200 μl of normal saline, the TgCtwh3 WT and TgCtwh3 Δ*rop16*$_{I/III}$ group was injected with TgCtwh3 WT or TgCtwh3 Δ*rop16*$_{I/III}$ tachyzoites of varying numbers, respectively. The APP expression in hippocampus was evaluated by western blotting and protein expression was determined semi-quantitatively (A, B). Changes in appearance and posture of mice induced by TgCtwh3 WT and TgCtwh3 Δ*rop16*$_{I/III}$ infection (C). Data were represented as mean ± SD and were analyzed by one-way ANOVA followed by Bonferroni's post hoc test for multiple comparisons (n = 10 each group). *$P < 0.05$, * *$P < 0.01$, * **$P < 0.001$, * ** *$P < 0.0001$

4.2. TgCtwh3 Δrop16$_{I/III}$ strain induces neuron apoptosis in mouse hippocampus

To assess whether TgCtwh3 WT or TgCtwh3 Δ*rop16*$_{I/III}$ tachyzoites could induce hippocampal neuron apoptosis, we infected mice with above tachyzoites, then carried out histopathologic examination and apoptosis-related proteins detection. HE staining of brain tissue showed that in the control group the hippocampal zones were uniformly stained with intact tissue, neuron structure and clear nuclear membrane boundaries. On the contrary, in the TgCtwh3 WT group the hippocampal neurons were disorganized in the arrangement, decreased in the number, and had abnormally deep nuclei staining. Moreover, in the TgCtwh3 Δ*rop16*$_{I/III}$ group neurons were more disorganized in the arrangement and more deeply stained in nuclei (Fig. 2A). Similarly, Nissl staining showed that the number of positive cells in the hippocampal tissues in the TgCtwh3 Δ*rop16*$_{I/III}$ group was decreased more remarkable than that in the TgCtwh3 WT group (Fig. 2B, C). The results indicated that TgCtwh3 Δ*rop16*$_{I/III}$ acute infection could lead to hippocampal neurons morphological change and loss. To determine whether the neuronal reduction was related with apoptosis, we took the mice hippocampus of three groups to detect apoptosis-related proteins by protein blotting (Fig. 2D). The results showed that Cleaved-caspase 3 and Bax were enhanced most significantly in the TgCtwh3 Δ*rop16*$_{I/III}$ group among the three groups, while Bcl-2 decreased most markedly in the TgCtwh3 Δ*rop16*$_{I/III}$ group among the three groups (Fig. 2E, F, G), revealing that TgCtwh3 Δ*rop16*$_{I/III}$ induced neuronal apoptosis more than TgCtwh3

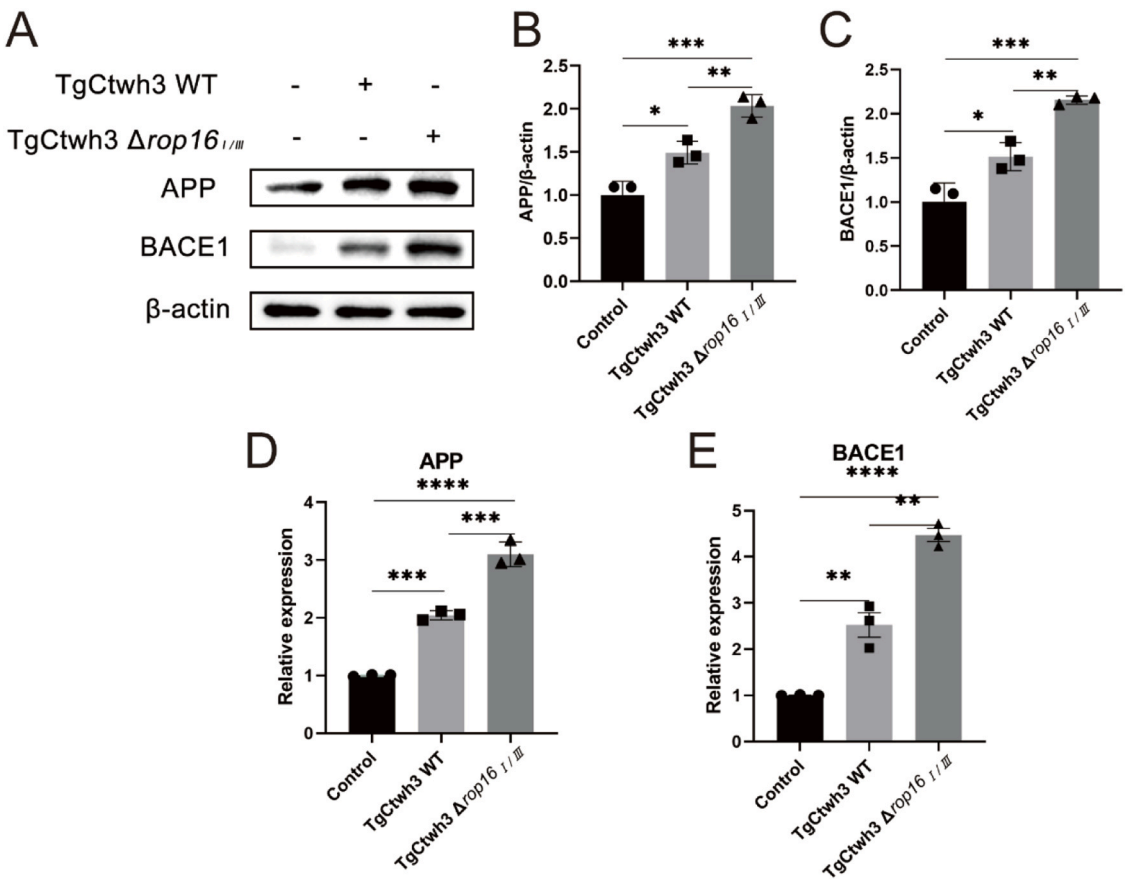

Fig. 3. TgCtwh3 Δ*rop16*$_{I/III}$ infection increased mouse hippocampal tissue APP, BACE1 expression.

WT in the hippocampal region.

The mouse hippocampal tissue was lysed, and then the tissue proteins were extracted. Apoptotic proteins were assessed by western blotting and protein expression was determined semi-quantitatively (D, E, F, G). The hippocampus tissue section was first stained with hematoxylin and eosin, and then was observed under a light microscope at a magnification of 20 × 10 and 40 × 10 (scale bars, 100μm, respectively) (A). Besides, the mouse hippocampus tissue section was stained with Nissl dye, and then was observed under a light microscope at a magnification of 40 × 10 (scale bars, 100μm) (B). The number of positive cells in each field of view was evaluated with semiquantitative analysis (C). Data were represented as mean ± SD and were analyzed by one-way ANOVA followed by Bonferroni's post hoc test for multiple comparisons (n = 3 each group). *$P < 0.05$, * *$P < 0.01$, * **$P < 0.001$, * ** *$P < 0.0001$

4.3. *TgCtwh3 Δrop16*$_{I/III}$ *strain induces APP and BACE1 expression in mouse hippocampus*

To verify the effect of TgCtwh3 Δ*rop16*$_{I/III}$ tachyzoite on the production of APP and BACE1, we detected mouse hippocampal tissue APP and BACE1 at protein and gene levels. Western blotting and qRT-PCR results showed that both APP and BACE1 expression rose most obviously in the TgCtwh3 Δ*rop16*$_{I/III}$ group among the three groups (Fig. 3A-E), implying that TgCtwh3 WT infection contributes to the production of APP and BACE1, moreover, TgCtwh3 Δ*rop16*$_{I/III}$ tachyzoite promotes APP and BACE1 production more than TgCtwh3 WT.

The mouse brain hippocampus tissues were lysed, then the tissue proteins were extracted; APP and BACE1 proteins were detected by western blotting and then analyzed semi-quantitatively (A–C). Finally, the RNA of the mouse hippocampus tissue was extracted and then reversely transcribed to cDNA. APP and BACE1 gene expressions were assessed by qRT-PCR and analyzed by semi-quantitative method (D, E). Data were represented as mean ± SD and were analyzed by one-way ANOVA followed by Bonferroni's post hoc test for multiple comparisons (n = 7 each group). *$P < 0.05$, * *$P < 0.01$, * **$P < 0.001$, * ** *$P < 0.0001$

4.4. *TgCtwh3 Δrop16*$_{I/III}$ *strain promotes pro-inflammatory factors secretion in mouse hippocampal tissue*

Inflammation is usually accompanied by secretion of pro-inflammatory factors. To identify whether TgCtwh3 infection can cause the secretion of pro-inflammatory factors in the hippocampal region of the mouse, we examined mouse hippocampal tissue iNOS, TNF-α, IL-6 and TGF-β1 at protein and gene levels. The results showed that the expression of pro-inflammatory factors iNOS, TNF-α and IL-6 was up-regulated most significantly in the TgCtwh3 Δ*rop16*$_{I/III}$ group among the three groups (Fig4A-D, F-H); on the contrary, the expression of anti-inflammatory factor TGF-β1 was down-regulated most notably in the TgCtwh3 Δ*rop16*$_{I/III}$ group among the three groups (Fig. 4A, E, I). Compared with the TgCtwh3 WT group, the expression of pro-inflammatory factors was higher and the anti-inflammatory factor was lower in the TgCtwh3 Δ*rop16*$_{I/III}$ group.

The mice hippocampal tissues were lysed, then the tissue proteins were extracted, followed by western blotting to detect inflammatory factors iNOS, IL-6, TNF-α, and TGF-β1 proteins with semiquantitative analysis (A-E). The RNA from mouse hippocampal tissues was extracted and reversely transcribed to cDNA. The gene expression of IL-6, TNF-α, iNOS, and TGF-β1 was assessed by qRT-PCR, followed by semi-quantitative analysis (F-I). Data were represented as mean ± SD and were analyzed by one-way ANOVA followed by Bonferroni's post hoc

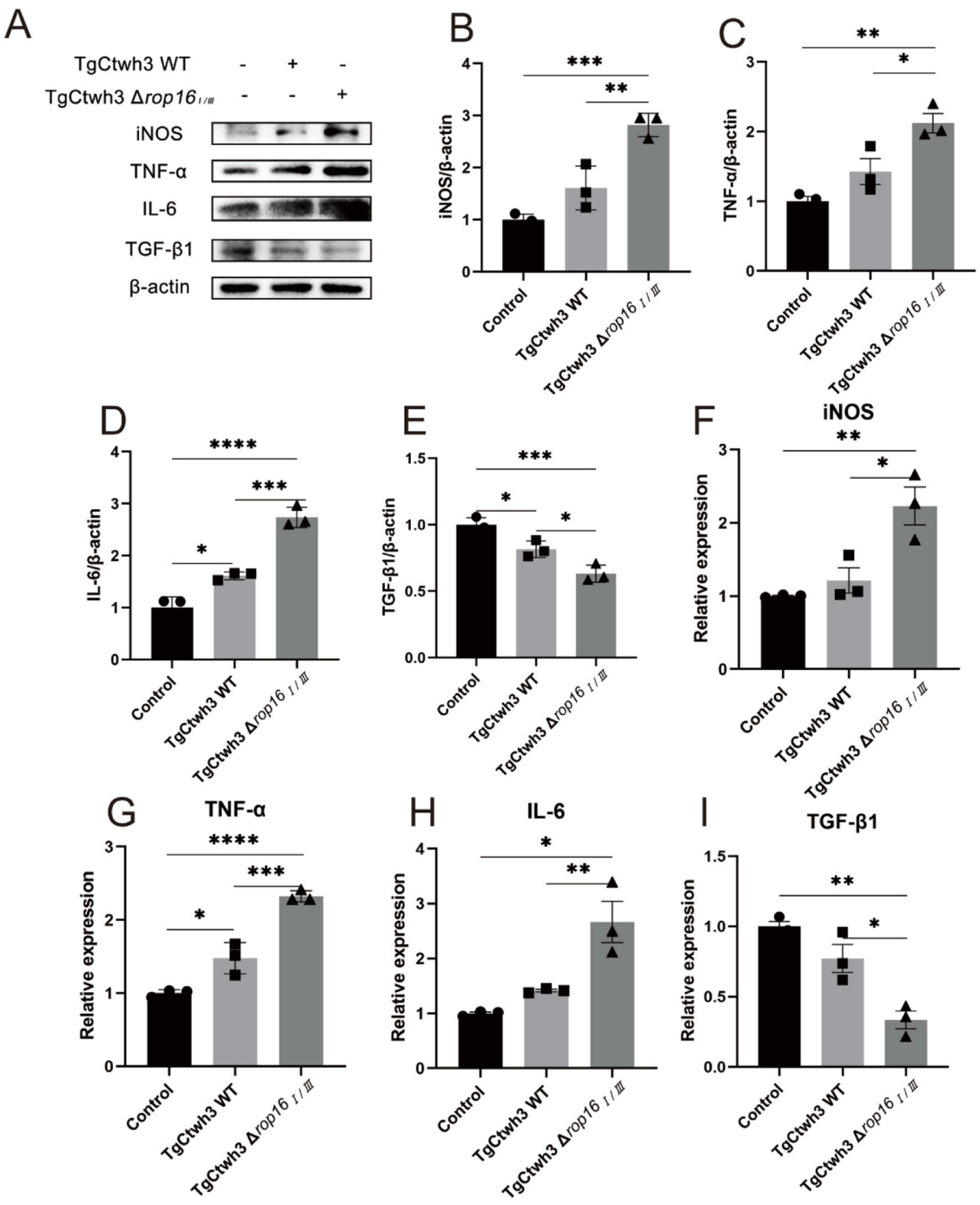

Fig. 4. Pro-inflammatory cytokines secretion was induced in mouse hippocampus by TgCtwh3 Δ*rop16*$_{I/III}$ infection.

test for multiple comparisons (n = 7 each group). *$P < 0.05$, * *$P < 0.01$, * **$P < 0.001$, * ** *$P < 0.0001$

4.5. *TgCtwh3 Δrop16*$_{I/III}$ *strain infection directly results in HT22 apoptosis*

To further clarify whether TgCtwh3 Δ*rop16*$_{I/III}$ tachyzoites could directly give rise to neuron apoptosis, we infected HT22, a mouse hippocampal neuron cell line, with TgCtwh3 WT and TgCtwh3 Δ*rop16*$_{I/III}$ tachyzoites to investigate *in vitro* the neuron apoptosis mechanism.

Firstly, the TgCtwh3 WT and TgCtwh3 Δ*rop16*$_{I/III}$ tachyzoites were cultured with HT22, respectively, for 24 h, and then the apoptosis-related proteins of HT22, such as Cleaved-caspase3, Bax and Bcl-2 were detected by western blotting. The results showed that the expression of pro-apoptotic proteins Cleaved-caspase3 and Bax was significantly highest; however, the expression of anti-apoptotic protein Bcl-2 was significantly lowest in the TgCtwh3 Δ*rop16*$_{I/III}$ group among the three groups (Fig. 5A-D). In addition, the flow cytometry results showed that the apoptosis rate was raised most significantly in the TgCtwh3 Δ*rop16*$_{I/III}$ group among the three groups (Fig. 5E, F). In our study, apoptotic cells were explicitly defined as the Annexin V+PI- population, whereas Annexin V+PI+ cells were considered to be late apoptotic/necrotic. The results indicated that TgCtwh3 Δ*rop16*$_{I/III}$ could directly induce HT22 apoptosis, which was the reason that TgCtwh3 Δ*rop16*$_{I/III}$ acute infection led to mouse hippocampal neurons morphological change and loss in our *in vivo* experiment.

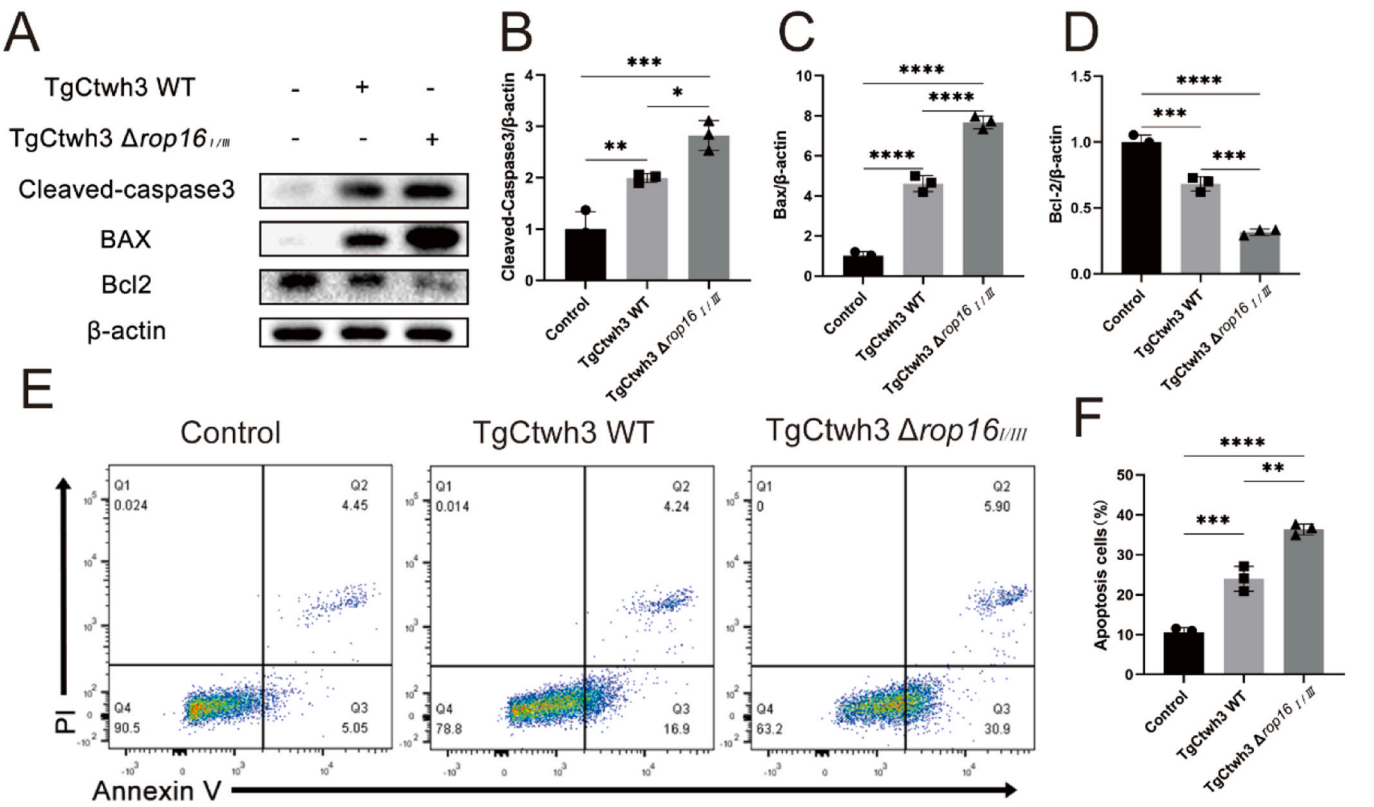

Fig. 5. HT22 apoptosis was caused by TgCtwh3 Δ*rop16*$_{I/III}$ infection.

After TgCtwh3 WT and TgCtwh3 Δ*rop16*$_{I/III}$ tachyzoites infected HT22, respectively, for 24 h, the HT22 were lysed and the cell proteins were extracted. The expression of apoptosis-related proteins of HT22, such as Cleaved-caspase3, Bax and Bcl-2 was measured by western blotting and then analyzed by semiquantitative method (A–D). In addition, the infected HT22 were collected to assess apoptotic status by flow cytometry (E, F). Data were represented as mean ± SD and were analyzed by one-way ANOVA followed by Bonferroni's post hoc test for multiple comparisons (n = 5 each group). *$P < 0.$ 05, * *$P < 0.01$, * **$P < 0.001$, * ** *$P < 0.0001$

4.6. TgCtwh3 Δrop16$_{I/III}$ strain increases APP and BACE1 expression in HT22

To investigate whether TgCtwh3 Δ*rop16*$_{I/III}$ could directly promote the production of APP and BACE1 in HT22, the protein levels of APP and BACE1 in HT22 infected with TgCtwh3 WT and TgCtwh3 Δ*rop16*$_{I/III}$ tachyzoites, respectively, were evaluated by western blotting and immunofluorescence staining. The results displayed that the level of APP and BACE1 in infected HT22 increased most remarkably in the TgCtwh3 Δ*rop16*$_{I/III}$ group among the three groups (Fig. 6A-C). In addition, the immunofluorescence results showed that the expression of APP and BACE1 protein-positive cells was up-regulated most markedly in the TgCtwh3 Δ*rop16*$_{I/III}$ group among the three groups (Fig. 6D-G). The results indicated that TgCtwh3 Δ*rop16*$_{I/III}$ could directly promote the production of APP and BACE1 in HT22.

After infection of HT22 with TgCtwh3 WT and TgCtwh3 Δ*rop16*$_{I/III}$ tachyzoites for 24 h, HT22 was lysed and the proteins were extracted. The expression of BACE1 and APP protein was detected by protein blotting and then analyzed by semiquantitative methods (A-C). In addition, BACE1 and APP proteins were visualized in situ by immunofluorescence staining and observed under a fluorescence microscope at 40 × 10 (scale bar, 100μm) after HT22 cells were fixed and the cell membranes were penetrated by Triton. The percentage of positively stained cells was calculated using morphometric software (D-G). Data were represented as mean ± SD and were analyzed by one-way ANOVA followed by Bonferroni's post hoc test for multiple comparisons (n = 5 each group). *$P < 0.$ 05, * *$P < 0.01$, * **$P < 0.001$, * ** *$P < 0.0001$

4.7. TgCtwh3 Δrop16$_{I/III}$ strain induces HT22 apoptosis through the ERS pathway

To further investigate the mechanism by which HT22 apoptosis was induced by TgCtwh3 Δ*rop16*$_{I/III}$, we used TUDCA to suppress ERS and then surveyed whether TgCtwh3 Δ*rop16*$_{I/III}$ could trigger the HT22 apoptosis via ERS pathway. HT22 were pretreated with 200 μM TUDCA for 12 h and then cultured with or without TgCtwh3 WT or TgCtwh3 Δ*rop16*$_{I/III}$ tachyzoites (MOI=3) for another 24 h. Western blotting results showed that the expression of immunoglobulin heavy chain-binding protein (BIP), Cleaved-caspase12 and Cleaved-caspase3 was most significantly elevated, respectively, in the TgCtwh3 Δ*rop16*$_{I/III}$ group without pretreatment among the six groups, whereas the expression of BIP, Cleaved-caspase12 and Cleaved-caspase3 was significantly reduced in the TUDCA pretreated group compared to that in the group without pretreatment (Fig. 7A-D). In addition, our flow cytometry results demonstrated that pretreatment with TUDCA significantly decreased the apoptotic rate in both TgCtwh3 WT and TgCtwh3 Δrop16I/III groups compared to untreated conditions(Fig. 7E, F).

The results implied that TgCtwh3, especially the TgCtwh3 Δ*rop16*$_{I/III}$ strain infection could induce ERS-mediated apoptosis pathway which promoted HT22 apoptosis.

HT22 were infected with TgCtwh3 WT or TgCtwh3 Δ*rop16*$_{I/III}$ tachyzoites for 24 h with or without TUDCA pretreatment. HT22 were lysed and then the cell proteins were extracted. The expression of BIP, Cleaved-caspase12, and Cleaved-caspase3 was detected by immunoblotting and then analyzed semi-quantitatively (A-D). In addition, HT22 were collected and the apoptosis rate was assessed by flow cytometry (E, F). Data were represented as mean ± SD and were analyzed by one-way

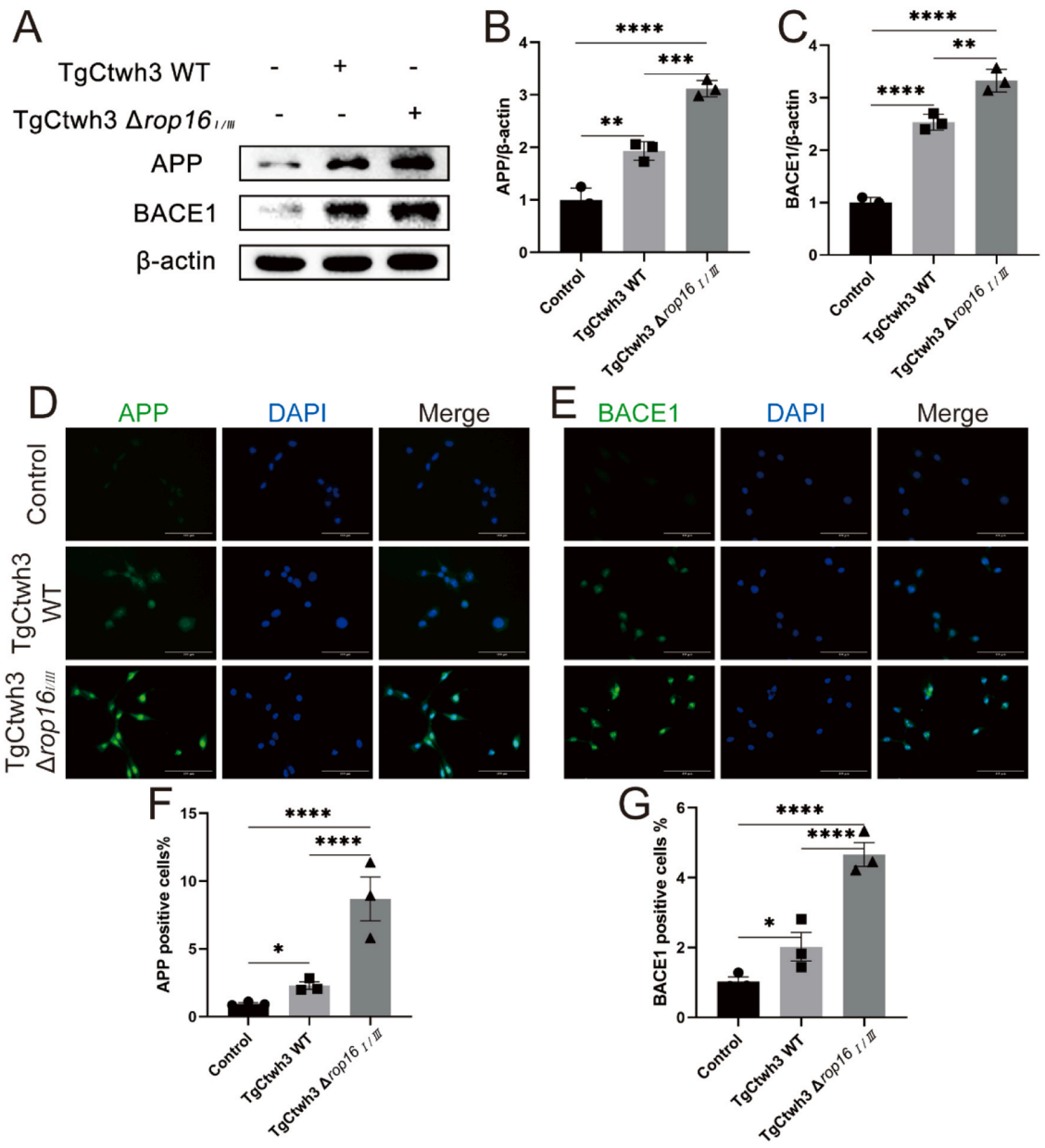

Fig. 6. Expression of APP and BACE1 in HT22 was directly facilitated by TgCtwh3 Δ*rop16*$_{I/III}$.

ANOVA followed by Bonferroni's post hoc test for multiple comparisons (n = 5 each group). *$P < 0.05$, * *$P < 0.01$, * **$P < 0.001$, * ** *$P < 0.0001$

4.8. *TgCtwh3 Δrop16*$_{I/III}$ *strain stimulates APP and BACE1 production in HT22 through NF-κB signaling pathway*

To further investigate the mechanism by which TgCtwh3 Δ*rop16*$_{I/III}$ tachyzoites induce APP and BACE1 production in HT22, we evaluated the effect of TgCtwh3 Δ*rop16*$_{I/III}$ on the generation of APP, BACE1, *p*-NF-κBp65 and NF-κBp65 in HT22 with or without JSH-23 pretreatment. HT22 pre-treated with or without 10 μM JSH-23 for 12 h were cultured with or without TgCtwh3 WT or TgCtwh3 Δ*rop16*$_{I/III}$ tachyzoites (MOI=3) for another 24 h. The western blotting results showed that the expression of APP, BACE1, NF-κBp65 and *p*-NF-κBp65 in the JSH-23-pretreated TgCtwh3 Δ*rop16*$_{I/III}$ group was significantly lower than that in the un-pretreated TgCtwh3 Δ*rop16*$_{I/III}$ group, respectively (Fig. 8A-E). Similarly, the immunofluorescence staining results manifested that the level of APP, BACE1, NF-κBp65 and *p*-NF-κBp65 in the un-pretreated TgCtwh3 Δ*rop16*$_{I/III}$ group was enhanced more evidently compared to that in the pretreated TgCtwh3 Δ*rop16*$_{I/III}$ group, respectively (Fig. 8F-M). Thus, both western blotting and immunofluorescence staining indicated that TgCtwh3 Δ*rop16*$_{I/III}$ tachyzoites stimulated APP and BACE1 production through directly facilitating NF-κB signaling in HT22.

HT22 were pretreated with or without JSH-23 and then infected with or without TgCtwh3 WT or TgCtwh3 Δ*rop16*$_{I/III}$. After HT22 was collected and lysed, the cell proteins were extracted. The expression of NF-κBp65, *p*-NF-κBp65, APP and BACE1 was detected by western blotting followed by semiquantitative analysis (A-E). In addition, the expression of NF-κBp65, *p*-NF-κBp65, APP and BACE1 was shown by immunofluorescence staining after HT22 were fixed and permeabilized by Triton penetration and visualized under a fluorescence microscope at 40 × 10. The percentage of positively stained cells was calculated using morphometric software (F-M). Data were represented as mean ± SD and were analyzed by one-way ANOVA followed by Bonferroni's post hoc test for multiple comparisons (n = 5 each group). *$P < 0.05$, * *$P < 0.01$, * **$P < 0.001$, * ** *$P < 0.0001$

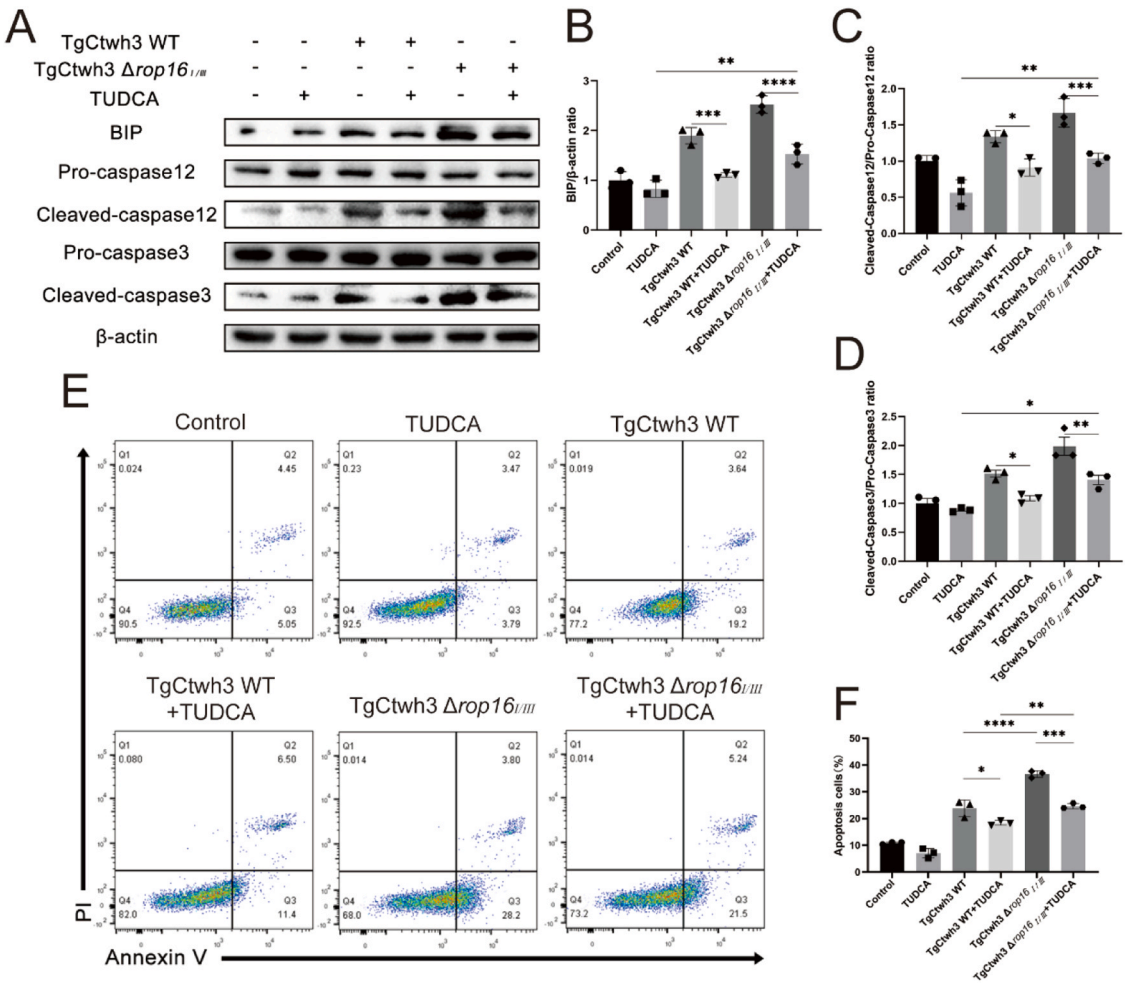

Fig. 7. HT22 apoptosis was promoted by TgCtwh3 Δ*rop16*$_{I/III}$ through ERS pathway.

5. Discussion

A growing body of evidence indicates to a strong correlation between *T.gondii* infection and neurodegenerative disorders, such as Alzheimer's disease (Tao et al., 2023; Xiao et al., 2022). Our previous research has shown that the TgCtwh6 tachyzoites can lead to mouse chronic infection and cognitive behavioral impairments with neuronal apoptosis, Aβ formation, and the secretion of pro-inflammatory factors (Tao et al., 2023). While the majority of mice infected with TgCtwh3 experience acute illnesses and succumb within two weeks (Li et al., 2014), but both TgCtwh3 and TgCtwh6 cause chronic infection in the population of China (Wang et al., 2015). As we know, ROP16$_{I/III}$ and GRA15$_{II}$ are the key virulence components of *T. gondii* (Hernandez-de-Los-Rios et al., 2019), and both of the two virulent effectors are present in *T. gondii* of the Chinese1 genotype (Cheng et al., 2015). So, in our present experiments, we infected mice and HT22 with TgCtwh3 WT and TgCtwh3 Δ*rop16*$_{I/III}$, respectively, to evaluate the effect of the TgCtwh3 Δ*rop16*$_{I/III}$ strain with *gra15*$_{II}$ background on neurons and explore its potential mechanism.

Following *T.gondii* infects mouse, *T.gondii* can cross the blood-brain barrier and enter the central nervous system, where it primarily targets neurons, meanwhile activating astrocytes and microglia to induce pro-inflammatory cytokines secretion which may cause neuronal loss and apoptosis (Cabral et al., 2016). In addition, in type II strains, GRA15$_{II}$ directly activates the NF-κB signaling pathway leading to a pro-inflammatory Th1-type immune response in brain, which contributes to neuronal apoptosis, APP, BACE1 production and neurodegenerative diseases development (Calsolaro and Edison, 2016; Leng and Edison, 2021; Matta et al., 2021; Novoa et al., 2022; Rani et al., 2023; Rosowski et al., 2011; Singh and Singh, 2020; Xie et al., 2018).

Our previous study has identified that GRA15$_{II}$ effector induced M1 polarization in RAW264.7 cells through NF-κB signaling and activated M1 produced pro-inflammatory factors (Xie et al., 2018). Our other study has further demonstrated that TgCtwh3 Δ*rop16*$_{I/III}$ strain infection significantly elevated the expression of Th1 cytokines and IL-17A in splenocytes and placental tissues in pregnant mouse (Wang et al., 2018). Our present study showed that TgCtwh3 Δ*rop16*$_{I/III}$ strain could significantly promote the expression of iNOS, TNF-α and IL-6; meanwhile remarkably reduced the expression of TGF-β1 in mouse hippocampal tissues. This result suggests that *gra15*$_{II}$ plays an important role in brain tissue pro-inflammatory response of mice acutely infected with TgCtwh3 Δ*rop16*$_{I/III}$ tachyzoites.

Previous research has demonstrated that *Toxoplasma*-mediated apoptosis is essential for the development of neurodegenerative lesions (Dincel and Atmaca, 2016). In our present study, we found abnormal arrangement and reduced number of hippocampal neurons with aberrant deep-stained nuclei in the TgCtwh3 Δ*rop16*$_{I/III}$ infection group, suggesting neuronal dysfunction and loss or apoptosis. Further research found that the expression of pro-apoptosis proteins Cleaved-caspase3 and Bax increased, while the expression of anti-apoptosis protein Bcl-2 decreased in the infected groups, especially in the TgCtwh3 Δ*rop16*$_{I/III}$ group, indicating that the neuron loss in acute infected mouse might be partially due to neuronal apoptosis.

Some researchers have found that TgCtwh3 WT could induce neural stem cell strain apoptosis via ERS signaling (Zhou et al., 2015); Another researchers have reported that *T.gondii* GRA15$_{II}$ could initiate

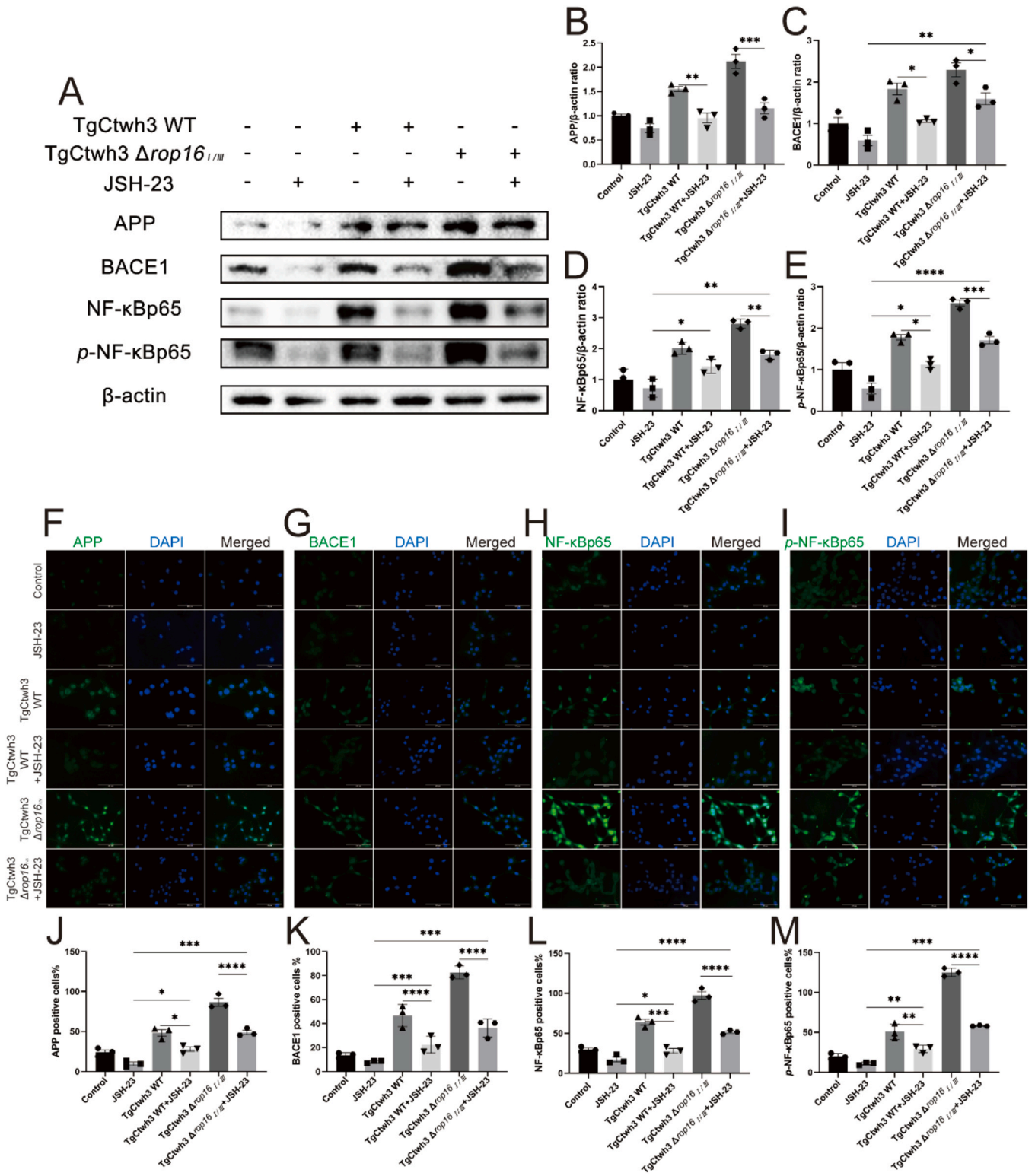

Fig. 8. APP and BACE1 expression were elevated in HT22 by TgCtwh3 Δ*rop16*$_{I/III}$ through promoting NF-κB signaling.

choriocarcinoma JEG-3 cells apoptosis through ERS (Wei et al., 2018). ERS-mediated apoptosis pathway has been recently identified as a mechanism that contributes to the development and progression of neurodegenerative illnesses (Ariyasu et al., 2017; Yang et al., 2015). Our present experiments showed that TgCtwh3 Δ*rop16*$_{I/III}$ could activate the ERS-mediated apoptosis through increasing the expression of BIP, Cleaved-caspase12 and Cleaved-caspase3, suggesting that GRA15$_{II}$ might induce neuronal apoptosis via ERS pathway. Additionally, it has been reported that ERS increases γ-secretase activity by up-regulating presenilin 1 (PSEN1) expression and therefore it might be implicated in Aβ peptide formation (Penke et al., 2017).

Aβ is produced by protein hydrolysis of the transmembrane protein APP by BACE1 and γ-secretase (Chen et al., 2017). Studies have indicated that NF-κB signaling plays a crucial role in the production of APP,

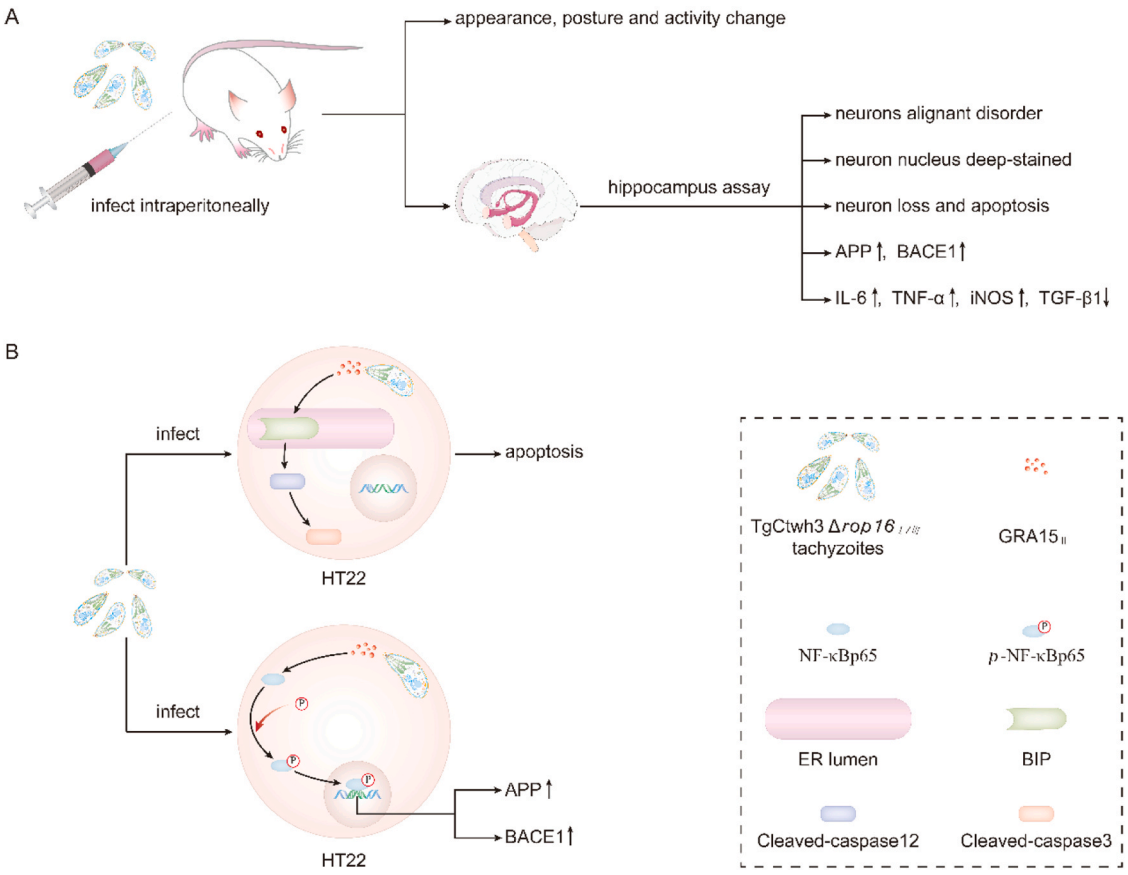

Fig. 9. Mechanism with which TgCtwh3 Δ*rop16*$_{I/III}$ tachyzoite induces neuron apoptosis and APP production in mouse with acute infection at the cellular and molecular level in our experiments.

BACE1and Aβ, elevated expression of APP and BACE1 in the brains of AD patients has been associated with increased NF-κB signaling pathway activation (Chen et al., 2012; Kim et al., 2021; Shi et al., 2017). It has been shown that the p65 subunit of NF-κB binds to the κB element of the BACE1 promoter, leading to increased expression of β-secretase (Chen et al., 2012). Moreover, *T. gondii* GRA15$_{II}$ can directly activate NF-κB pathway (Rosowski et al., 2011). In our study, infection of HT22 with TgCtwh3 Δ*rop16*$_{I/III}$ resulted in up-regulation of NF-κBp65 and *p*-NF-κBp65, along with APP and BACE1 expressions, however, JSH-23 reversed up-regulation of these expressions which suggested that TgCtwh3 Δ*rop16*$_{I/III}$ tachyzoite infection could lead to APP and BACE1 production through the NF-κB signaling pathway, and *gra15*$_{II}$ might play a major role in this process.

In summary, in our experiment we infected intraperitoneally mouse with 1000 TgCtwh3 Δ*rop16*$_{I/III}$ tachyzoites. One week following infection, the infected mouse presented abnormal appearance and posture changes as well as declined vitality. The hippocampus assay demonstrated that TgCtwh3 Δ*rop16*$_{I/III}$ *toxoplasma* with *gra15*$_{II}$ background caused neuron loss, neuron alignment disorder, neuronal nucleus abnormal deep-stained and neuron apoptosis. Moreover, TgCtwh3 Δ*rop16*$_{I/III}$ tachyzoite accelerated APP, BACE1 production and pro-inflammatory cytokines secretion in hippocampal tissue of acute infected mouse. To make clear the mechanics of the neuron apoptosis and APP, BACE1 production induced by TgCtwh3 Δ*rop16*$_{I/III}$ tachyzoite, we carried out the *in vitro* cytologic experiment, which suggested that TgCtwh3 Δ*rop16*$_{I/III}$ induced neural apoptosis via ERS pathway; meanwhile, TgCtwh3 Δ*rop16*$_{I/III}$ initiated APP and BACE1 production through NF-κB signaling (Fig. 9). Obviously, *gra15*$_{II}$ might play a key role in this course. This study would be helpful for us to better understand the genotype-associated mechanism of protein aggregation-related disorder, such as AD, caused by *Toxoplasma* predominantly prevalent in China. In the future, *gra15*$_{II}$ might become a promising targeted molecule in prevention and therapy of AD patients who has been infected with *T.gondii* type Chinese1 strains. We will further verify our speculation in our future work using primary hippocampal cultured neurons; furthermore, we will use biochip and in situ hybridization histochemistry.

First, *in vivo*, BALB/c mouse was infected intraperitoneally with TgCtwh3 Δ*rop16*$_{I/III}$ tachyzoite. One week later, the infected mouse presented abnormal appearance and posture changes as well as declined vigour. The infected mouse hippocampal tissue assay showed that neurons were disorganized in the arrangement, decreased in the number and abnormally stained in nuclei. Moreover, TgCtwh3 Δ*rop16*$_{I/III}$ tachyzoite accelerated APP, BACE1 production and pro-inflammatory cytokines secretion in hippocampal tissue of acute infected mouse (A). TgCtwh3 Δ*rop16*$_{I/III}$ tachyzoite led to HT22 apoptosis via ERS pathway, and promoted APP, BACE1 production in HT22 through NF-κB signaling (B).

Abbreviations

AD: Alzheimer's disease; APP: Amyloid precursor protein; Aβ: Beta-amyloid; BACE1: β-secretase 1; BIP: immunoglobulin heavy chain-binding protein; DAPI: 2-(4-Amidinophenyl)-6-indolecarbamidine dihydrochloride; DMEM: Dulbecco's modifed Eagle's medium; ERS: endoplasmic reticulum stress; FBS: Fetal bovine serum; FCM: Flow cytometry; FITC: fluorescein isothiocyanate; GRA: dense granules protein; GRA15$_{II}$: type II *T. gondii* GRA 15 protein; H&E: Hematoxylin and eosin; HT22: Mouse hippocampal neuronal cell line; IL-6: interleukin-6; iNOS: inducible nitric oxide sythase; JSH-23: 4-Methyl-N1- (3-phenylpropyl) −1,2-phenylenediamine;MOI: Multiplicity of Infection; PMSF: phenylmethanesulfonyl fluoride; PSEN1: presenilin 1; PVDF:

polyvinylidene difluoride membrane; qRT-PCR: real-time quantitative PCR; ROP: rhoptry protein; ROP16$_{I/III}$: Type I or III *T.gondii* ROP16 protein; SPF: Specific Pathogen Free; TgCtwh3: *Toxoplasma gondii* Chinese 1 genotype Wh3 strain; TgCtwh3 WT: TgCtwh3 wild type; TgCtwh3 Δ*rop16*:*rop16*$_{I/III}$-deficient/*gra15*$_{II}$-dominant toxoplasma gondii Chinese 1 genotype Wh3; TgCtwh6: *Toxoplasma gondii* Chinese 1 genotype Wh6 strain; *T.gondii*: *Toxoplasma gondii*; TGF-β1: transforming growth factor beta 1; Th1: type 1 helper; TNF: tumor necrosis factor; TUDCA: Tauroursodeoxycholate

CRediT authorship contribution statement

Deyong Chu, Kunpeng Qin and Jilong Shen designed the experiments; Di Yang, Qing Tao, Cong Wang, Lei Liu and Mengtao Gong conducted the experiments; Mengmeng Jin, Haiping Cai, Qingli Luo and Meijuan Zheng performed the test and statistical analyses; Di Yang wrote this manuscript. Deyong Chu, Jilong Shen, Jian Du, and Li Yu edited the manuscript. All authors read and approved the final manuscript.

Ethics approval and consent to participate

Animal procedures were approved by the Institutional Review Board of the Institute of Biomedicine at Anhui Medical University (permit number: AMU26093628).

Consent for publication

Not applicable.

Funding

This work was supported by the Provincial University Natural Science Research Key Project of Anhui (No. kJ2019A0222).

Declaration of Competing Interest

The authors declare that they have no known competing financial interests or personal relationships that could have appeared to influence the work reported in this paper.

Acknowledgements

We thank the assistant of the Center for Scientific Research of Anhui Medical University.

Data Availability

All articles from which data was cited to support the conclusions of this manuscript are listed in the text and the reference.

References

Ariyasu, D., Yoshida, H., Hasegawa, Y., 2017. Endoplasmic reticulum (ER) stress and endocrine disorders. Int J. Mol. Sci. 18.
Caballero, E., Hernando-Perez, E., Tapias, V., Calvo-Rodriguez, M., Villalobos, C., Nunez, L., 2022. Amyloid beta oligomers-induced Ca(2+) ENtry Pathways: Role of Neuronal Networks, Nmda Receptors and Amyloid Channel Formation. Biomedicines 10.
Cabral, C.M., Tuladhar, S., Dietrich, H.K., Nguyen, E., MacDonald, W.R., Trivedi, T., Devineni, A., Koshy, A.A., 2016. Neurons are the primary target cell for the brain-tropic intracellular parasite Toxoplasma gondii. PLoS Pathog. 12, e1005447.
Calsolaro, V., Edison, P., 2016. Neuroinflammation in Alzheimer's disease: current evidence and future directions. Alzheimers Dement 12, 719–732.
Catumbela, C.S.G., Giridharan, V.V., Barichello, T., Morales, R., 2023. Clinical evidence of human pathogens implicated in Alzheimer's disease pathology and the therapeutic efficacy of antimicrobials: an overview. Transl. Neurodegener. 12, 37.
Chen, G.F., Xu, T.H., Yan, Y., Zhou, Y.R., Jiang, Y., Melcher, K., Xu, H.E., 2017. Amyloid beta: structure, biology and structure-based therapeutic development. Acta Pharm. Sin. 38, 1205–1235.
Chen, C.H., Zhou, W., Liu, S., Deng, Y., Cai, F., Tone, M., Tone, Y., Tong, Y., et al., 2012. Increased NF-kappaB signalling up-regulates BACE1 expression and its therapeutic potential in Alzheimer's disease. Int J. Neuropsychopharmacol. 15, 77–90.
Cheng, W., Liu, F., Li, M., Hu, X., Chen, H., Pappoe, F., Luo, Q., Wen, H., et al., 2015. Variation detection based on next-generation sequencing of type Chinese 1 strains of Toxoplasma gondii with different virulence from China. BMC Genom. 16, 888.
Dincel, G.C., Atmaca, H.T., 2016. Increased expressions of ADAMTS-13 and apoptosis contribute to neuropathology during Toxoplasma gondii encephalitis in mice. Neuropathology 36, 211–226.
Dubey, J.P., Lindsay, D.S., Speer, C.A., 1998. Structures of Toxoplasma gondii tachyzoites, bradyzoites, and sporozoites and biology and development of tissue cysts. Clin. Microbiol Rev. 11, 267–299.
Dugger, B.N., Dickson, D.W., 2017. Pathology of neurodegenerative diseases. Cold Spring Harb. Perspect. Biol. 9.
El Saftawy, E.A., Amin, N.M., Sabry, R.M., El-Anwar, N., Shash, R.Y., Elsebaie, E.H., Wassef, R.M., 2020. Can Toxoplasma gondii pave the road for dementia? J. Parasitol. Res 2020, 8859857.
Graham, G.J., Pragnell, I.B., 1990. Negative regulators of haemopoiesis–current advances. Prog. Growth Factor Res 2, 181–192.
Guglielmotto, M., Monteleone, D., Boido, M., Piras, A., Giliberto, L., Borghi, R., Vercelli, A., Fornaro, M., et al., 2012. Abeta1-42-mediated down-regulation of Uch-L1 is dependent on NF-kappaB activation and impaired BACE1 lysosomal degradation. Aging Cell 11, 834–844.
Hernandez-de-Los-Rios, A., Murillo-Leon, M., Mantilla-Muriel, L.E., Arenas, A.F., Vargas-Montes, M., Cardona, N., de-la-Torre, A., Sepulveda-Arias, J.C., et al., 2019. Influence of Two Major Toxoplasma Gondii Virulence Factors (ROP16 and ROP18) on the Immune Response of Peripheral Blood Mononuclear Cells to Human Toxoplasmosis Infection. Front Cell Infect. Microbiol 9, 413.
Howe, D.K., Sibley, L.D., 1995. Toxoplasma gondii comprises three clonal lineages: correlation of parasite genotype with human disease. J. Infect. Dis. 172, 1561–1566.
Huang, R., Hui, Z., Wei, S., Li, D., Li, W., Daping, W., Alahdal, M., 2022. IRE1 signaling regulates chondrocyte apoptosis and death fate in the osteoarthritis. J. Cell Physiol. 237, 118–127.
Jensen, K.D., Wang, Y., Wojno, E.D., Shastri, A.J., Hu, K., Cornel, L., Boedec, E., Ong, Y. C., et al., 2011. Toxoplasma polymorphic effectors determine macrophage polarization and intestinal inflammation. Cell Host Microbe 9, 472–483.
Kim, B., Lee, K.Y., Park, B., 2021. Isoorientin inhibits amyloid beta(25-35)-induced neuronal inflammation in BV2 cells by blocking the NF-kappaB signaling pathway. Molecules 26.
Kinney, J.W., Bemiller, S.M., Murtishaw, A.S., Leisgang, A.M., Salazar, A.M., Lamb, B.T., 2018. Inflammation as a central mechanism in Alzheimer's disease. Alzheimers Dement (N. Y 4, 575–590.
Leng, F., Edison, P., 2021. Neuroinflammation and microglial activation in Alzheimer disease: where do we go from here? Nat. Rev. Neurol. 17, 157–172.
Li, M., Mo, X.W., Wang, L., Chen, H., Luo, Q.L., Wen, H.Q., Wei, W., Zhang, A.M., et al., 2014. Phylogeny and virulence divergency analyses of Toxoplasma gondii isolates from China. Parasit. Vectors 7, 133.
Liu, Z., Liu, G., Ha, D.P., Wang, J., Xiong, M., Lee, A.S., 2023. ER chaperone GRP78/BiP translocates to the nucleus under stress and acts as a transcriptional regulator. Proc. Natl. Acad. Sci. USA 120, e2303448120.
Liu, Y., Wen, D., Gao, J.Q., Xie, B., Yu, H.L., Shen, Q.C., Zhang, J.J., Jing, W.W., et al., 2020. Methamphetamine induces GSDME-dependent cell death in hippocampal neuronal cells through the endoplasmic reticulum stress pathway. Brain Res. Bull. 162, 73–83.
Matta, S.K., Rinkenberger, N., Dunay, I.R., Sibley, L.D., 2021. Toxoplasma gondii infection and its implications within the central nervous system. Nat. Rev. Microbiol 19, 467–480.
Nakagawa, T., Zhu, H., Morishima, N., Li, E., Xu, J., Yankner, B.A., Yuan, J., 2000. Caspase-12 mediates endoplasmic-reticulum-specific apoptosis and cytotoxicity by amyloid-beta. Natura 403, 98–103.
Novoa, C., Salazar, P., Cisternas, P., Gherardelli, C., Vera-Salazar, R., Zolezzi, J.M., Inestrosa, N.C., 2022. Inflammation context in Alzheimer's disease, a relationship intricate to define. Biol. Res 55, 39.
Oakley, H., Cole, S.L., Logan, S., Maus, E., Shao, P., Craft, J., Guillozet-Bongaarts, A., Ohno, M., et al., 2006. Intraneuronal beta-amyloid aggregates, neurodegeneration, and neuron loss in transgenic mice with five familial Alzheimer's disease mutations: potential factors in amyloid plaque formation. J. Neurosci. 26, 10129–10140.
Olivera, G.C., Ross, E.C., Peuckert, C., Barragan, A., 2021. Blood-brain barrier-restricted translocation of Toxoplasma gondii from cortical capillaries. Elife 10.
Peng, D., Li, J., Deng, Y., Zhu, X., Zhao, L., Zhang, Y., Li, Z., Ou, S., et al., 2020. Sodium para-aminosalicylic acid inhibits manganese-induced NLRP3 inflammasome-dependent pyroptosis by inhibiting NF-kappaB pathway activation and oxidative stress. J. Neuroinflamm. 17, 343.
Penke, B., Bogar, F., Fulop, L., 2017. beta-Amyloid and the Pathomechanisms of Alzheimer's Disease: A Comprehensive View. Molecules 22.
Pfaffenbach, K.T., Lee, A.S., 2011. The critical role of GRP78 in physiologic and pathologic stress. Curr. Opin. Cell Biol. 23, 150–156.
Piekut, T., Hurla, M., Banaszek, N., Szejn, P., Dorszewska, J., Kozubski, W., Prendecki, M., 2022. Infectious agents and Alzheimer's disease. J. Integr. Neurosci. 21, 73.

Rani, V., Verma, R., Kumar, K., Chawla, R., 2023. Role of pro-inflammatory cytokines in Alzheimer's disease and neuroprotective effects of pegylated self-assembled nanoscaffolds. Curr. Res Pharm. Drug Discov. 4, 100149.
Rao, R.V., Hermel, E., Castro-Obregon, S., del Rio, G., Ellerby, L.M., Ellerby, H.M., Bredesen, D.E., 2001. Coupling endoplasmic reticulum stress to the cell death program. Mech. caspase Act. J. Biol. Chem. 276, 33869–33874.
Rosowski, E.E., Lu, D., Julien, L., Rodda, L., Gaiser, R.A., Jensen, K.D., Saeij, J.P., 2011. Strain-specific activation of the NF-kappaB pathway by GRA15, a novel Toxoplasma gondii dense granule protein. J. Exp. Med 208, 195–212.
Saeij, J.P., Boyle, J.P., Coller, S., Taylor, S., Sibley, L.D., Brooke-Powell, E.T., Ajioka, J. W., Boothroyd, J.C., 2006. Polymorphic secreted kinases are key virulence factors in toxoplasmosis. Science 314, 1780–1783.
Shi, Z., Chen, T., Yao, Q., Zheng, L., Zhang, Z., Wang, J., Hu, Z., Cui, H., et al., 2017. The circular RNA ciRS-7 promotes APP and BACE1 degradation in an NF-kappaB-dependent manner. FEBS J. 284, 1096–1109.
Singh, S., Singh, T.G., 2020. Role of Nuclear Factor Kappa B (NF-kappaB) Signalling in Neurodegenerative Diseases: An Mechanistic Approach. Curr. Neuropharmacol. 18, 918–935.
Tao, Q., Yang, D., Qin, K., Liu, L., Jin, M., Zhang, F., Zhu, J., Wang, J., et al., 2023. Studies on the mechanism of Toxoplasma gondii Chinese 1 genotype Wh6 strain causing mice abnormal cognitive behavior. Parasit. Vectors 16, 30.
Taylor, S., Barragan, A., Su, C., Fux, B., Fentress, S.J., Tang, K., Beatty, W.L., Hajj, H.E., et al., 2006. A secreted serine-threonine kinase determines virulence in the eukaryotic pathogen Toxoplasma gondii. Science 314, 1776–1780.
Tseng, C.C., Zhang, P., Lee, A.S., 2019. The COOH-terminal proline-rich region of GRP78 is a key regulator of its cell surface expression and viability of tamoxifen-resistant breast cancer cells. Neoplasia 21, 837–848.
Vidal, C.M., Ouyang, C., Qi, Y., Mendez-Dorantes, C., Coblentz, A., Alva-Ornelas, J.A., Stark, J.M., Seewaldt, V.L., et al., 2023. Arginine regulates HSPA5/BiP translation through ribosome pausing in triple-negative breast cancer cells. Br. J. Cancer 129, 444–454.
Wang, C., Cheng, W., Yu, Q., Xing, T., Chen, S., Liu, L., Yu, L., Du, J., et al., 2018. Toxoplasma Chinese 1 strain of WH3Deltarop16(I/III) /gra15(II) genetic background contributes to abnormal pregnant outcomes in murine model. Front Immunol. 9, 1222.
Wang, L., He, L.Y., Meng, D.D., Chen, Z.W., Wen, H., Fang, G.S., Luo, Q.L., Huang, K.Q., et al., 2015. Seroprevalence and genetic characterization of Toxoplasma gondii in cancer patients in Anhui Province, Eastern China. Parasit. Vectors 8, 162.
Wei, W., Zhang, F., Chen, H., Tang, Y., Xing, T., Luo, Q., Yu, L., Du, J., et al., 2018. Toxoplasma gondii dense granule protein 15 induces apoptosis in choriocarcinoma JEG-3 cells through endoplasmic reticulum stress. Parasit. Vectors 11, 251.
Xiao, J., Savonenko, A., Yolken, R.H., 2022. Strain-specific pre-existing immunity: A key to understanding the role of chronic Toxoplasma infection in cognition and Alzheimer's diseases? Neurosci. Biobehav Rev. 137, 104660.
Xie, Y., Wen, H., Yan, K., Wang, S., Wang, X., Chen, J., Li, Y., Xu, Y., et al., 2018. Toxoplasma gondii GRA15(II) effector-induced M1 cells ameliorate liver fibrosis in mice infected with Schistosomiasis japonica. Cell Mol. Immunol. 15, 120–134.
Xu, Y.W., Xing, R.X., Zhang, W.H., Li, L., Wu, Y., Hu, J., Wang, C., Luo, Q.L., et al., 2019. Toxoplasma ROP16(I/III) ameliorated inflammatory bowel diseases via inducing M2 phenotype of macrophages. World J. Gastroenterol. 25, 6634–6652.
Yang, Y.Z., Sun, M., Shan, Y.Y., Zheng, X.M., Ma, H.M., Ma, W.Z., Wang, Z.S., Pei, X.Y., et al., 2015. Endoplasmic Reticulum Stress-Mediated Apoptotic Pathway Is Involved in Corpus Luteum Regression in Rats. Reprod. Sci. 22, 572–584.
Zhou, J., Gan, X., Wang, Y., Zhang, X., Ding, X., Chen, L., Du, J., Luo, Q., et al., 2015. Toxoplasma gondii prevalent in China induce weaker apoptosis of neural stem cells C17.2 via endoplasmic reticulum stress (ERS) signaling pathways. Parasit. Vectors 8, 73.
Zhou, B., Lu, J.G., Siddu, A., Wernig, M., Sudhof, T.C., 2022. Synaptogenic effect of APP-Swedish mutation in familial Alzheimer's disease. Sci. Transl. Med 14, eabn9380.